

Efficient Multi-view Clustering via Unified and Discrete Bipartite Graph Learning

Si-Guo Fang, Dong Huang, Xiao-Sha Cai, Chang-Dong Wang, Chaobo He, and Yong Tang

Abstract—Although previous graph-based multi-view clustering algorithms have gained significant progress, most of them are still faced with three limitations. First, they often suffer from high computational complexity, which restricts their applications in large-scale scenarios. Second, they usually perform graph learning either at the single-view level or at the view-consensus level, but often neglect the possibility of the joint learning of single-view and consensus graphs. Third, many of them rely on the k -means for discretization of the spectral embeddings, which lack the ability to directly learn the graph with discrete cluster structure. In light of this, this paper presents an efficient multi-view clustering approach via unified and discrete bipartite graph learning (UDBGL). Specifically, the anchor-based subspace learning is incorporated to learn the view-specific bipartite graphs from multiple views, upon which the bipartite graph fusion is leveraged to learn a view-consensus bipartite graph with adaptive weight learning. Further, the Laplacian rank constraint is imposed to ensure that the fused bipartite graph has discrete cluster structures (with a specific number of connected components). By simultaneously formulating the view-specific bipartite graph learning, the view-consensus bipartite graph learning, and the discrete cluster structure learning into a unified objective function, an efficient minimization algorithm is then designed to tackle this optimization problem and directly achieve a discrete clustering solution without requiring additional partitioning, which notably has linear time complexity in data size. Experiments on a variety of multi-view datasets demonstrate the robustness and efficiency of our UDBGL approach.

Index Terms—Data clustering, Multi-view clustering, Large-scale clustering, Bipartite graph learning, Linear time.

I. INTRODUCTION

WITH the continuous development of information technology, an increasing amount of data can be collected from multiple sources (or views) in real-world scenarios, which is often referred to as multi-view data [1]. For example, an image can be depicted by different feature descriptors, such as local binary pattern (LBP), histogram of oriented gradient (HOG), and Gabor descriptor. A piece of news can be described in different languages, such as Chinese, English, and Spanish. To effectively utilize the multi-view information

for the clustering task, many multi-view clustering (MVC) methods have been developed in the literature, among which the graph-based methods have attracted significant research attention in recent years.

The graph-based MVC methods [2]–[8] typically build (or learn) some graph structure(s) to reflect the sample-wise relationships in multi-view data, and then partition the graph to obtain the clustering result. A general strategy is to formulate the sample-wise relationships into an $n \times n$ adjacent graph, where n is the number of samples. Wang et al. [4] utilized a mutual reinforcement technique to learn the single-view graphs and a unified global graph. Liang et al. [5], [9] leveraged both the consistency and inconsistency of multiple single-view graphs, and learned a unified graph via multi-view graph learning. Besides these graph learning based methods [4]–[6], [9], another popular sub-category of the graph-based MVC methods are the subspace learning based methods [10]–[15], which seek to learn a self-representation matrix from low-dimensional subspaces and further utilize the learned self-representation matrix as a global similarity graph for final clustering. Cao et al. [16] proposed a multi-view subspace clustering method via smoothness and diversity, with the complementarity of multiple representations investigated. Chen et al. [17] enabled the simultaneous learning of the latent embedding space, the global self-representation, and the cluster structures for multi-view subspace learning. Despite the rapid progress, yet these methods mostly suffer from high computational complexity, where the construction of an $n \times n$ adjacent graph typically consumes $\mathcal{O}(n^2)$ time and the spectral partitioning of this graph may even take $\mathcal{O}(n^3)$ time, which restrict their computational feasibility for large datasets.

To breakthrough the computational bottleneck, the bipartite graph (i.e., anchor graph) based MVC methods [18]–[28] have recently shown promising capability. Instead of relying on some $n \times n$ graph, the bipartite graph based methods typically generate a small set of anchors from the original data and then construct an $n \times m$ bipartite graph to represent the data structure, where m is the number of anchors. Specifically, Kang et al. [27] learned a bipartite graph for each view via the anchor-based subspace learning, and then heuristically concatenated the multiple bipartite graphs into a unified one. Wang et al. [26] learned a unified bipartite graph for all views via a set of latent consensus anchors and multiple projection matrices. However, these bipartite graph-based methods [25]–[27] either (i) learn a single bipartite graph for all views [25], [26] or (ii) learn a bipartite graph for each view and then concatenate these multiple graphs heuristically [27], which lack the ability to simultaneously

This work was supported by the NSFC (61976097, 61876193, 62077045, & U1811263) and the Natural Science Foundation of Guangdong Province (2021A1515012203). (Corresponding author: Dong Huang.)

S.-G. Fang and D. Huang are with the College of Mathematics and Informatics, South China Agricultural University, Guangzhou, China. E-mail: siguofang@hotmail.com, huangdonghere@gmail.com.

X.-S. Cai and C.-D. Wang are with the School of Computer Science and Engineering, Sun Yat-sen University, Guangzhou, China, and also with Guangdong Key Laboratory of Information Security Technology, Guangzhou, China. E-mail: xiaoshacai@hotmail.com, changdongwang@hotmail.com.

C. He and Y. Tang are with the School of Computer Science, South China Normal University, Guangzhou, China. E-mail: hechaobo@foxmail.com, ytang@m.scnu.edu.cn.

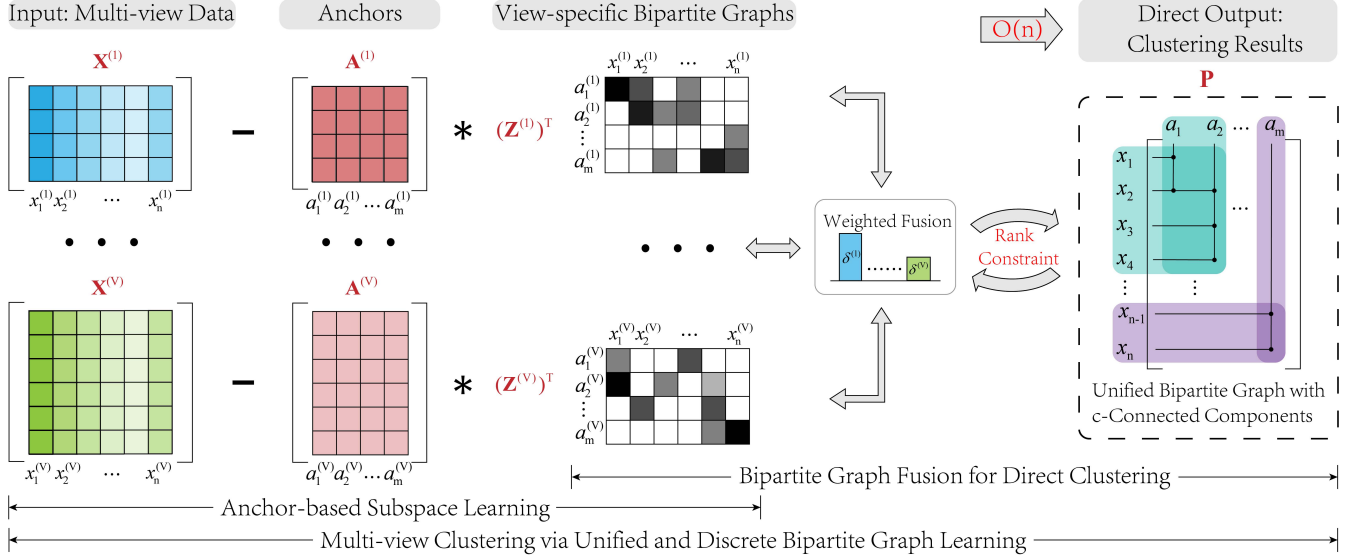


Fig. 1. Illustration of our UDBGL framework. In the anchor-based subspace learning, multiple view-specific bipartite graphs are learned via the self-expressive loss. In the bipartite graph fusion, UDBGL learns the view-consensus bipartite graph with c -connected components and adaptive weights. The view-specific bipartite graph learning (via anchor-based subspace learning) and the view-consensus bipartite graph learning are simultaneously performed and mutually promoted by each other, whose computational complexity is linear to n .

formulate the view-specific bipartite graph learning and the view-consensus bipartite graph learning. Moreover, they often regard the bipartite graph learning and its partitioning as two separate phases, and cannot directly obtain the clustering result by learning a bipartite graph with discrete cluster structure. More recently, Li et al. [22] proposed a scalable multi-view clustering method via bipartite graph fusion. Although it is able to adaptively learn a unified graph with discrete cluster structure by fusing multiple view-specific bipartite graphs, yet these view-specific bipartite graphs are pre-constructed and cannot be adaptively optimized. Despite these recent advances, it is still a challenging problem how to enable the unified learning of the view-specific bipartite graphs and the view-consensus bipartite graph, while ensuring the discrete cluster structure of the learned graph and maintaining the efficiency of the overall framework for large-scale datasets.

To address the above-mentioned problem, this paper presents an efficient multi-view clustering approach via **unified and discrete bipartite graph learning (UDBGL)**. Particularly, the anchor-based subspace learning is utilized to learn the view-specific bipartite graphs (for multiple views), which are fused into a view-consensus bipartite graph that in turn promotes the view-specific bipartite graph learning. During the fusion, the view weights are adaptively learned to balance the influences of different view-specific bipartite graphs. Furthermore, we impose a Laplacian rank constraint on the unified bipartite graph so as to directly obtain the desired number of connected components, which leads to the discrete cluster structure without requiring additional partitioning. Notably, the view-specific bipartite graph learning, the view-consensus bipartite graph learning, and the discrete cluster structure learning are seamlessly incorporated into a unified objective function, upon which an efficient alternating optimization algorithm is designed to achieve the final clustering with almost

linear computational complexity. Experiments are conducted on eight real-world multi-view datasets, which confirm the superiority of our UDBGL approach over the state-of-the-art.

For clarity, the main contributions of this work are summarized as follows:

- This paper bridges the gap between the view-specific bipartite graph learning and the view-consensus bipartite graph learning, which can be promoted by each other mutually and adaptively during their learning.
- A unified objective function is presented to encompass the view-specific and view-consensus bipartite graph learning and the discrete cluster structure learning, to solve which a *linear-time* optimization algorithm is further designed.
- An efficient MVC approach termed UDBGL is proposed. Experiments on multiple multi-view datasets demonstrate the clustering robustness and scalability of our UDBGL approach over the state-of-the-art MVC approaches.

The remainder of the paper is arranged as follows. Section II reviews the related works. Section III describes the formulation of our UDBGL approach. Section IV presents the optimization algorithm and its complexity analysis. Section V reports the experimental results. Finally, Section VI concludes this paper.

II. RELATED WORK

This paper focuses on efficient MVC with unified and discrete bipartite graph learning. Therefore, in this section, our literature review pays attention to three main issues in MVC, namely, how to fuse multiple similarity graphs (from multiple views) into a unified similarity graph, how to build and fuse the similarity graphs with high efficiency (for large datasets), and how to learn the graph with discrete cluster structure without additional partitioning process.

In terms of graph learning (or graph fusion), a variety of MVC methods have been proposed, which aim to fuse

the similarity relationships among data samples in multiple views into a unified graph. Zhan et al. [3] adopted the rank constraint of the Laplacian matrix and the graph regularization to learn the unified graph from the multiple single-view graphs. Wang et al. [4] fused multiple single-view graphs into a unified one, and in turn optimized the single-view graphs through the unified graph. Liang et al. [5], [9] simultaneously and explicitly modeled the consistency and inconsistency in multiple single-view graphs and fused them via an efficient optimization algorithm.

In terms of the computational complexity, some bipartite graph-based methods have been proposed, which, instead of building an $n \times n$ graph, resort to an $n \times m$ bipartite graph, where $m \ll n$ is the number of anchors, so as to make them computationally feasible for large-scale datasets. Nie et al. [19] aimed to learn an optimal bipartite graph with ideal connected components for co-clustering. Further, Nie et al. [24] utilized a dictionary matrix to learn a structured optimal bipartite graph via subspace clustering with the Laplacian rank constraint, which is designed for the single-view situation. For the multi-view situations, Sun et al. [25] proposed a unified bipartite graph learning model with view-unified and orthogonal anchors, where view-specific weights are adaptively learned. In addition, the bipartite graph could also be utilized to reconstruct point-to-point relationships for incomplete multi-view clustering [20].

In terms of the direct (or discrete) clustering, these aforementioned methods mostly learn or build a unified graph and then conduct additional spectral partitioning on the graph to obtain the final clustering. However, the spectral partitioning (i.e., spectral clustering) often requires performing the k -means clustering on the spectral embeddings, which may bring in performance degradation due to the instability of k -means. To this end, some previous works incorporate the Laplacian rank constraint to learn a graph with discrete cluster structure, which can direct lead to the clustering result without performing additional partitioning [3], [22], [24], but still lack the ability to unify the single-view and unified bipartite graph learning in a joint learning model.

III. METHODOLOGY

In this section, we present the formulation of the proposed UDBGL approach. Specifically, Section III-A introduces the main notations used throughout the paper. The view-specific subspace learning with anchors is represented in Section III-B. The Laplacian rank-constrained bipartite graph fusion is formulated in Section III-C. Finally, Section III-D describes the overall framework of UDBGL.

A. Notations

Throughout this paper, we denote the scalar values by italic letters, the vectors by boldface lower-case letters, and the matrices by boldface capital letters. The j -th column of matrix \mathbf{M} is written as $\mathbf{m}_{:,j}$ (or $\mathbf{M}(:,j)$), with its i -th entry being $m_{i,j}$ (or $\mathbf{M}(i,j)$). $\|\mathbf{v}\|_2$ denotes the 2-norm of a vector \mathbf{v} , and $\|\mathbf{M}\|_F$ denotes the Frobenius norm of matrix \mathbf{M} . $\mathbf{v} \geq 0$ (or $\mathbf{M} \geq 0$) represents that all of the entries in this vector (or this matrix)

TABLE I
NOTATIONS

Notations	Descriptions
n	The number of samples
c	The number of clusters
V	The number of views
m	The number of anchors
$d^{(v)}$	The number of features in the v -th view
$\mathbf{X}^{(v)} \in \mathbb{R}^{d^{(v)} \times n}$	Data matrix in the v -th view
$\mathbf{Z}^{(v)} \in \mathbb{R}^{n \times m}$	View-specific bipartite graph of the v -th view
$\mathbf{P} \in \mathbb{R}^{n \times m}$	View-consensus bipartite graph
$\mathbf{A}^{(v)} \in \mathbb{R}^{d^{(v)} \times m}$	Anchor matrix in the v -th view
$\boldsymbol{\delta} \in \mathbb{R}^V$	$[\delta^{(1)}, \delta^{(2)}, \dots, \delta^{(V)}]^\top$ The view coefficient vector

are larger than or equal to zero. \mathbf{I} denotes the identity matrix. $\mathbf{1}$ denotes a column vector with all entries being one. For clarity, Table III-A shows some frequently-used notations and their descriptions.

B. View-specific Subspace Learning with Anchors

Let a single-view data matrix be denoted as $\mathbf{X} \in \mathbb{R}^{d \times n}$, which consists of n samples with d features. According to sparse subspace clustering (SSC) [12], it is assumed that a data point can be written as a linear or affine combination of all other data points, i.e., $\mathbf{X} = \mathbf{X}\mathbf{Z}^\top + \mathbf{E}$, where $\mathbf{Z} \in \mathbb{R}^{n \times n}$ is the self-representation matrix with the constraint $z_{ii} = 0$ to enforce that each point cannot be represented by itself, and $\mathbf{E} \in \mathbb{R}^{d \times n}$ is the error term. It aims to minimize the error term to find a better self-representation matrix, whose objective function can be written as

$$\begin{aligned} \min_{\mathbf{Z}} \quad & \|\mathbf{X} - \mathbf{X}\mathbf{Z}^\top\|_F^2 + \alpha \|\mathbf{Z}\|_F^2, \\ \text{s.t.} \quad & \mathbf{Z} \geq 0, \mathbf{Z}\mathbf{1} = \mathbf{1}; \forall i, z_{ii} = 0, \end{aligned} \quad (1)$$

where $\|\mathbf{Z}\|_F^2$ is the regularization term that prevents the model from the trivial solution, and $\alpha > 0$ is a hyper-parameter to control the influence of the regularization term. By constraining $\mathbf{Z} \geq 0, \mathbf{Z}\mathbf{1} = \mathbf{1}$, the elements in \mathbf{Z} with $0 \leq z_{ij} \leq 1$ can represent the similarity between the i -th point and the j -th point. Thus \mathbf{Z} can also be regarded as a similarity graph.

For multi-view subspace clustering, it is challenging to fuse information from different views due to the potential inconsistency among multiple views [10]. Let $\mathbf{X}^{(v)} \in \mathbb{R}^{d^{(v)} \times n}$ denote the v -th data matrix of the multi-view dataset, where $d^{(v)}$ is the number of features in the v -th view. Thus, we can perform the subspace learning on every single view as

$$\begin{aligned} \min_{\mathbf{Z}^{(v)}} \quad & \sum_{v=1}^V \left\{ \left\| \mathbf{X}^{(v)} - \mathbf{X}^{(v)}(\mathbf{Z}^{(v)})^\top \right\|_F^2 + \alpha \left\| \mathbf{Z}^{(v)} \right\|_F^2 \right\}, \\ & + \beta \mathcal{F}(\mathbf{Z}^{(1)}, \dots, \mathbf{Z}^{(V)}), \\ \text{s.t.} \quad & \mathbf{Z}^{(v)} \geq 0, \mathbf{Z}^{(v)}\mathbf{1} = \mathbf{1}; \forall v, i, z_{ii}^{(v)} = 0, \end{aligned} \quad (2)$$

where $\mathcal{F}(\mathbf{Z}^{(1)}, \dots, \mathbf{Z}^{(V)})$ is a regularization term which enforces the consistency of multiple self-representation matrices

$\mathbf{Z}^{(v)} \in \mathbb{R}^{n \times n}$, and $\beta > 0$ is a hyper-parameter to control the influence of the regularization term.

The above-mentioned model needs to learn multiple $n \times n$ graphs, which takes at least $\mathcal{O}(n^2)$ time. Recently, it has proved to be a promising strategy to use the anchor graph (i.e., bipartite graph) rather than using the $n \times n$ graph [22], [27]. Specifically, a straightforward way to construct the anchors is to conduct the k -means clustering on the concatenated features and then split the obtained centers (i.e., anchors) of the concatenated features by views [28]. Let $[\mathbf{A}^{(1)}; \mathbf{A}^{(2)}; \dots; \mathbf{A}^{(V)}] \in \mathbb{R}^{\sum_v d^{(v)} \times m}$ denote the anchor matrix for the dataset $[\mathbf{X}^{(1)}; \mathbf{X}^{(2)}; \dots; \mathbf{X}^{(V)}] \in \mathbb{R}^{\sum_v d^{(v)} \times n}$, where $\mathbf{A}^{(v)}$ is the anchor matrix for the v -th view and m is the number of anchors. We extend the objective (2) from the conventional subspace learning to the anchor-based subspace learning by replacing the data matrix $\mathbf{X}^{(v)}$ with the anchor matrix $\mathbf{A}^{(v)}$, and thus rewrite the objective function as

$$\begin{aligned} \min_{\mathbf{Z}^{(v)}} \sum_{v=1}^V \left\{ \left\| \mathbf{X}^{(v)} - \mathbf{A}^{(v)} (\mathbf{Z}^{(v)})^\top \right\|_F^2 + \alpha \left\| \mathbf{Z}^{(v)} \right\|_F^2 \right\}, \\ + \beta \mathcal{F}(\mathbf{Z}^{(1)}, \dots, \mathbf{Z}^{(V)}), \\ \text{s.t. } \mathbf{Z}^{(v)} \geq 0, \mathbf{Z}^{(v)} \mathbf{1} = \mathbf{1}, \end{aligned} \quad (3)$$

where the representation matrix $\mathbf{Z}^{(v)} \in \mathbb{R}^{n \times m}$ can be interpreted as a bipartite graph between the n original samples and the m anchors.

C. Rank-constrained Bipartite Graph Fusion

In this section, we proceed to fuse multiple bipartite graphs from multiple views into a unified bipartite graph. Notably, the multiple bipartite graphs are associated with adaptively-learned weights, and a Laplacian rank constraint is further imposed for learning a unified bipartite graph with discrete cluster structure.

Formally, the objective function for bipartite graph fusion can be formulated as

$$\begin{aligned} \min_{\mathbf{P}, \boldsymbol{\delta}} \left\| \sum_{v=1}^V \delta^{(v)} \mathbf{Z}^{(v)} - \mathbf{P} \right\|_F^2, \\ \text{s.t. } \boldsymbol{\delta}^\top \mathbf{1} = 1, \boldsymbol{\delta} \geq 0; \mathbf{P} \in \boldsymbol{\Omega}, \end{aligned} \quad (4)$$

where $\boldsymbol{\delta} = [\delta^{(1)}, \delta^{(2)}, \dots, \delta^{(V)}]^\top$ is the view coefficient vector, and $\boldsymbol{\Omega} = \{\mathbf{P} \mid \mathbf{P} \mathbf{1} = \mathbf{1}, \mathbf{P} \geq 0\}$ ensures that $\mathbf{Z}^{(v)}$ and \mathbf{P} are at a similar scale.

After obtaining the unified bipartite graph \mathbf{P} , the traditional strategy is to approximately construct a similarity graph among all samples through the obtained bipartite graph. The doubly-stochastic similarity graph $\mathbf{S} \in \mathbb{R}^{n \times n}$ [20], [29], whose summation of each row or each column equals to 1, can be built as

$$\mathbf{S} = \mathbf{P} \boldsymbol{\Lambda}^{-1} \mathbf{P}^\top, \quad (5)$$

$$\boldsymbol{\Lambda} = \text{diag}(\mathbf{P}^\top \mathbf{1}) \in \mathbb{R}^{m \times m}, \quad (6)$$

where the $\text{diag}(\cdot)$ function returns a diagonal matrix whose main diagonal elements are the corresponding elements of input vector. Subsequently, the spectral clustering can be

conducted on the similarity graph \mathbf{S} , which takes at least $\mathcal{O}(n^2 c)$ time [27], where c is the desired number of clusters. Regarding this, we redefine the similarity graph \mathbf{S} in a different way from the aforementioned Eq. (5). That is

$$\mathbf{S} = \begin{pmatrix} \mathbf{P}^\top & \mathbf{P} \end{pmatrix} \in \mathbb{R}^{(n+m) \times (n+m)}. \quad (7)$$

Lemma 1. [22], [30] *Let \mathbf{S} be an undirected graph with non-negative elements. The multiplicity of the eigenvalue 0 of the normalized Laplacian matrix $\tilde{\mathbf{L}}_{\mathbf{S}}$ equals the number of connected components in the graph \mathbf{S} .*

In order to reduce the time complexity and directly achieve the discrete cluster structure without additional partitioning, we impose a rank constraint on the normalized Laplacian matrix (i.e., $\text{rank}(\tilde{\mathbf{L}}_{\mathbf{S}}) = n + m - c$) of the similarity graph \mathbf{S} , where $\tilde{\mathbf{L}}_{\mathbf{S}} = \mathbf{I} - \mathbf{D}_{\mathbf{S}}^{-\frac{1}{2}} \mathbf{S} \mathbf{D}_{\mathbf{S}}^{-\frac{1}{2}}$ is the normalized Laplacian matrix, and $\mathbf{D}_{\mathbf{S}} = \text{diag}(\mathbf{S} \mathbf{1}) \in \mathbb{R}^{(n+m) \times (n+m)}$ is the degree matrix. According to Lemma 1, the rank constraint enforces that the multiplicity of eigenvalue 0 of $\tilde{\mathbf{L}}_{\mathbf{S}}$ should be c , which leads to the learned graph \mathbf{S} with exact c connected components.

Further, since \mathbf{S} and \mathbf{P} represent the same graph, the c -connected components of the bipartite graph \mathbf{P} are guaranteed through the c -connected graph \mathbf{S} . Thus the constraints on \mathbf{P} can be rewritten as

$$\boldsymbol{\Omega} = \{\mathbf{P} \mid \mathbf{P} \mathbf{1} = \mathbf{1}, \mathbf{P} \geq 0; \text{rank}(\tilde{\mathbf{L}}_{\mathbf{S}}) = n + m - c\}. \quad (8)$$

Through the Laplacian rank constraint, the final clustering result can be directly gained from \mathbf{P} without additional partitioning. Thereby, we rewrite the objective function of the bipartite graph fusion as follows:

$$\begin{aligned} \min_{\mathbf{P}, \boldsymbol{\delta}} \left\| \sum_{v=1}^V \delta^{(v)} \mathbf{Z}^{(v)} - \mathbf{P} \right\|_F^2, \\ \text{s.t. } \boldsymbol{\delta}^\top \mathbf{1} = 1, \boldsymbol{\delta} \geq 0; \mathbf{P} \mathbf{1} = \mathbf{1}, \mathbf{P} \geq 0; \text{rank}(\tilde{\mathbf{L}}_{\mathbf{S}}) = n + m - c. \end{aligned} \quad (9)$$

D. Multi-view Clustering via Unified and Discrete Bipartite Graph Learning

Though previous MVC methods based on bipartite graph learning have achieved considerable progress, yet most of them *either* pre-construct the view-specific bipartite graphs and then learn a unified bipartite graph [18], [19], [22], [28] *or* learn multiple view-specific bipartite graphs and then simply concatenate the learned view-specific bipartite graphs into a unified one [27]. However, the pre-constructed bipartite graphs lack the ability of adaptive learning and refining, while the simple concatenation cannot well explore the latent structures of multiple bipartite graphs. Surprisingly, there remains a challenging gap between the view-specific bipartite graph learning and the view-consensus bipartite graph learning in most of previous works [18], [19], [22], [27], [28].

In this paper, we seek to unify the view-specific bipartite graph learning, the view-consensus bipartite graph learning, and the discrete cluster structure learning in a joint learning model. Particularly, the objective (3) (for anchor-based subspace learning) and the objective (9) are jointly formulated,

where the graph fusion objective serves as a regularization term for the objective (3) and the Laplacian rank constraint bridges the gap between the bipartite graph learning and the discrete cluster structure learning. Formally, the objective function for the unified and discrete bipartite graph learning can be formulated as follows:

$$\begin{aligned} \min_{\mathbf{Z}^{(v)}, \mathbf{P}, \delta} \quad & \sum_{v=1}^V \left\{ \left\| \mathbf{X}^{(v)} - \mathbf{A}^{(v)}(\mathbf{Z}^{(v)})^\top \right\|_F^2 + \alpha \left\| \mathbf{Z}^{(v)} \right\|_F^2 \right\} \\ & + \beta \left\| \sum_{v=1}^V \delta^{(v)} \mathbf{Z}^{(v)} - \mathbf{P} \right\|_F^2, \\ \text{s.t.} \quad & \mathbf{Z}^{(v)} \geq 0, \mathbf{Z}^{(v)} \mathbf{1} = \mathbf{1}; \delta^\top \mathbf{1} = 1, \delta \geq 0; \mathbf{P} \mathbf{1} = \mathbf{1}, \mathbf{P} \geq 0; \\ & \text{rank}(\tilde{\mathbf{L}}_{\mathbf{S}}) = n + m - c. \end{aligned} \quad (10)$$

In the next section, we will present a fast optimization algorithm to minimize this unified objective function, which enables the mutual promotion of the view-specific bipartite graphs and the view-consensus bipartite graph, and direct achieves the final clustering result without requiring additional graph partitioning.

IV. OPTIMIZATION AND COMPLEXITY ANALYSIS

In this section, we design an efficient alternating optimization algorithm to minimize the objective function (10). Specifically, in each iteration, we update each of the variables \mathbf{P} , $\mathbf{Z}^{(v)}$, and δ while fixing the other variables in Sections IV-A, IV-B and IV-C, respectively. The computational complexity of our proposed algorithm is further analyzed in Section IV-D.

A. Update \mathbf{P}

With the other variables fixed, the subproblem that only relates to \mathbf{P} can be written as

$$\begin{aligned} \min_{\mathbf{P}} \quad & \left\| \sum_{v=1}^V \delta^{(v)} \mathbf{Z}^{(v)} - \mathbf{P} \right\|_F^2, \\ \text{s.t.} \quad & \mathbf{P} \mathbf{1} = \mathbf{1}, \mathbf{P} \geq 0; \text{rank}(\tilde{\mathbf{L}}_{\mathbf{S}}) = n + m - c. \end{aligned} \quad (11)$$

According to [22] and the Ky Fan's Theorems [31], let $\mathbf{B} = \sum_{v=1}^V \delta^{(v)} \mathbf{Z}^{(v)}$, the subproblem (11) can be further transformed into

$$\begin{aligned} \min_{\mathbf{P}, \mathbf{F}} \quad & \left\| \mathbf{B} - \mathbf{P} \right\|_F^2 + \gamma \text{Tr}(\mathbf{F}^\top \tilde{\mathbf{L}}_{\mathbf{S}} \mathbf{F}), \\ \text{s.t.} \quad & \mathbf{P} \mathbf{1} = \mathbf{1}, \mathbf{P} \geq 0; \mathbf{F}^\top \mathbf{F} = \mathbf{I}, \end{aligned} \quad (12)$$

where $\mathbf{F} \in \mathbb{R}^{(n+m) \times c}$ is the indicator matrix, and γ can be automatically determined based on the number of connected components of \mathbf{P} . Further, we alternately optimize the variables \mathbf{F} and \mathbf{P} .

First, with \mathbf{P} fixed, the subproblem w.r.t. \mathbf{F} can be formulated as

$$\begin{aligned} \min_{\mathbf{F}^\top \mathbf{F} = \mathbf{I}} \quad & \text{Tr}(\mathbf{F}^\top \tilde{\mathbf{L}}_{\mathbf{S}} \mathbf{F}) \\ \Leftrightarrow \quad & \max_{\mathbf{F}_{(n)}^\top \mathbf{F}_{(n)} + \mathbf{F}_{(m)}^\top \mathbf{F}_{(m)} = \mathbf{I}} \text{Tr}(\mathbf{F}_{(n)}^\top \mathbf{D}_{(n)}^{-\frac{1}{2}} \mathbf{P} \mathbf{D}_{(m)}^{-\frac{1}{2}} \mathbf{F}_{(m)}), \end{aligned} \quad (13)$$

with

$$\mathbf{F} = \begin{pmatrix} \mathbf{F}_{(n)} \\ \mathbf{F}_{(m)} \end{pmatrix}, \mathbf{F}_{(n)} \in \mathbb{R}^{n \times c}, \mathbf{F}_{(m)} \in \mathbb{R}^{m \times c}, \quad (14)$$

$$\mathbf{D}_{\mathbf{S}} = \begin{pmatrix} \mathbf{D}_{(n)} & \\ & \mathbf{D}_{(m)} \end{pmatrix}, \mathbf{D}_{(n)} \in \mathbb{R}^{n \times n}, \mathbf{D}_{(m)} \in \mathbb{R}^{m \times m}, \quad (15)$$

According to [19], the optimal solutions to the problem (13) can be obtained as $\mathbf{F}_{(n)} = \frac{\sqrt{2}}{2} \mathbf{U}$ and $\mathbf{F}_{(m)} = \frac{\sqrt{2}}{2} \mathbf{V}$, where \mathbf{U} and \mathbf{V} are the largest c left and right singular vectors of $\mathbf{D}_{(n)}^{-\frac{1}{2}} \mathbf{P} \mathbf{D}_{(m)}^{-\frac{1}{2}}$, respectively.

Second, according to [22], we can have the following equality:

$$\text{Tr}(\mathbf{F}^\top \tilde{\mathbf{L}}_{\mathbf{S}} \mathbf{F}) = \sum_{i=1}^n \sum_{j=1}^m \left\| \frac{\mathbf{F}_{(n)}(i, :)}{\sqrt{\mathbf{D}_{(n)}(i, i)}} - \frac{\mathbf{F}_{(m)}(j, :)}{\sqrt{\mathbf{D}_{(m)}(j, j)}} \right\|_2^2 p_{ij}. \quad (16)$$

Let $q_{ij} = \left\| \frac{\mathbf{F}_{(n)}(i, :)}{\sqrt{\mathbf{D}_{(n)}(i, i)}} - \frac{\mathbf{F}_{(m)}(j, :)}{\sqrt{\mathbf{D}_{(m)}(j, j)}} \right\|_2^2$. With \mathbf{F} fixed, the subproblem w.r.t. \mathbf{P} can be written as

$$\min_{\mathbf{P} \mathbf{1} = \mathbf{1}, \mathbf{P} \geq 0} \sum_{i=1}^n \sum_{j=1}^m (b_{ij} - p_{ij})^2 + \gamma q_{ij} p_{ij}. \quad (17)$$

Because the optimization of each row of \mathbf{P} in the subproblem (17) is independent, we optimize \mathbf{P} by rows:

$$\min_{\mathbf{p}_i: \mathbf{1} = \mathbf{1}, \mathbf{p}_i \geq 0} \left\| \mathbf{p}_i - \left(\mathbf{b}_i - \frac{\gamma}{2} \mathbf{q}_i \right) \right\|_2^2. \quad (18)$$

Then the closed form solution \mathbf{p}_i can be obtained according to [32].

B. Update $\mathbf{Z}^{(v)}$

With the other variables fixed, the subproblem that only relates to $\mathbf{Z}^{(v)}$ can be written as

$$\begin{aligned} \min_{\mathbf{Z}^{(v)}} \quad & \left\| \mathbf{X}^{(v)} - \mathbf{A}^{(v)}(\mathbf{Z}^{(v)})^\top \right\|_F^2 + \alpha \left\| \mathbf{Z}^{(v)} \right\|_F^2 \\ & + \beta \left\| \sum_{i=1}^V \delta^{(i)} \mathbf{Z}^{(i)} - \mathbf{P} \right\|_F^2, \\ \text{s.t.} \quad & \mathbf{Z}^{(v)} \geq 0, \mathbf{Z}^{(v)} \mathbf{1} = \mathbf{1}. \end{aligned} \quad (19)$$

Since the optimization of each row of $\mathbf{Z}^{(v)}$ in the subproblem (19) is independent, we optimize $\mathbf{Z}^{(v)}$ by rows:

$$\begin{aligned} \min_{\mathbf{z}_{j:}^{(v)}} \quad & \left\| \mathbf{x}_{j:}^{(v)} - \mathbf{A}^{(v)}(\mathbf{z}_{j:}^{(v)})^\top \right\|_2^2 + \alpha \left\| \mathbf{z}_{j:}^{(v)} \right\|_2^2 \\ & + \beta \left\| \sum_{i=1}^V \delta^{(i)} \mathbf{z}_{j:}^{(i)} - \mathbf{p}_{j:} \right\|_2^2, \\ \text{s.t.} \quad & \mathbf{z}_{j:}^{(v)} \geq 0, \mathbf{z}_{j:}^{(v)} \mathbf{1} = 1. \end{aligned} \quad (20)$$

The above optimization problem (20) can be easily formulated as the following quadratic programming (QP) problem

$$\begin{aligned} \min_{\mathbf{z}_{j:}^{(v)}} \quad & \mathbf{z}_{j:}^{(v)} \mathbf{H}(\mathbf{z}_{j:}^{(v)})^\top + \mathbf{z}_{j:}^{(v)} \mathbf{f}, \\ \text{s.t.} \quad & \mathbf{z}_{j:}^{(v)} \geq 0, \mathbf{z}_{j:}^{(v)} \mathbf{1} = 1, \end{aligned} \quad (21)$$

where

$$\mathbf{H} = (\mathbf{A}^{(v)})^\top \mathbf{A}^{(v)} + \left(\alpha + \beta (\delta^{(v)})^2 \right) \mathbf{I},$$

$$\mathbf{f} = -2(\mathbf{A}^{(v)})^\top \mathbf{x}_{:,j}^{(v)} + 2\beta \delta^{(v)} \left(\sum_{i \neq v} \delta^{(i)} (\mathbf{z}_{j,:}^{(i)})^\top - \mathbf{p}_{j,:}^\top \right). \quad (22)$$

The problem (21) can be solved by using the augmented Lagrangian multiplier (ALM) [33] (please see the Section IV-C for the details).

C. Update δ

With the other variables fixed, the subproblem that only relates to δ can be written as

$$\min_{\delta} \left\| \sum_{v=1}^V \delta^{(v)} \mathbf{Z}^{(v)} - \mathbf{P} \right\|_F^2,$$

$$s.t. \quad \delta^\top \mathbf{1} = 1, \delta \geq 0. \quad (23)$$

In order to solve the subproblem (23), we vectorize each matrix $\mathbf{Z}^{(v)}$ into a vector $\hat{\mathbf{z}}^{(v)}$, that is

$$\hat{\mathbf{z}}^{(v)} = [\mathbf{z}_{:,1}^{(v)}; \mathbf{z}_{:,2}^{(v)}; \dots; \mathbf{z}_{:,m}^{(v)}] \in \mathbb{R}^{nm \times 1}, \quad (24)$$

where $\mathbf{z}_{:,i}^{(v)}$ represents the i -th column of $\mathbf{Z}^{(v)}$. Further, we stack the vectors $\hat{\mathbf{z}}^{(v)}$ for V views into a matrix $\hat{\mathbf{Z}} = [\hat{\mathbf{z}}^{(1)}; \hat{\mathbf{z}}^{(2)}; \dots; \hat{\mathbf{z}}^{(V)}] \in \mathbb{R}^{nm \times V}$. Note that $\mathbf{B} = \sum_{v=1}^V \delta^{(v)} \mathbf{Z}^{(v)}$, and $\hat{\mathbf{b}}$ is the vectorization of \mathbf{B} (similar to Eq. (24)), so we have $\hat{\mathbf{b}} = \hat{\mathbf{Z}}\delta$. Similarly, $\hat{\mathbf{p}}$ is the vectorization of \mathbf{P} , then the problem (23) can be rewritten as

$$\min_{\delta^\top \mathbf{1}=1, \delta \geq 0} \left\| \hat{\mathbf{Z}}\delta - \hat{\mathbf{p}} \right\|_2^2$$

$$\Leftrightarrow \min_{\delta^\top \mathbf{1}=1, \delta \geq 0} \delta^\top \mathbf{H} \delta - \delta^\top \mathbf{f}, \quad (25)$$

where $\mathbf{H} = \hat{\mathbf{Z}}^\top \hat{\mathbf{Z}}$, and $\mathbf{f} = 2\hat{\mathbf{Z}}^\top \hat{\mathbf{p}}$. The objective (25) is a convex quadratic programming with the semi-definite quadratic matrix \mathbf{H} . Here, we use the augmented Lagrangian multiplier (ALM) [33] to optimize the objective (25), whose solution is obtained by solving its equivalence:

$$\min_{\delta^\top \mathbf{1}=1, \delta \geq 0, \rho} \delta^\top \mathbf{H} \delta - \delta^\top \mathbf{f}. \quad (26)$$

The augmented Lagrangian function of the objective (26) can be written as:

$$\min_{\delta^\top \mathbf{1}=1, \delta \geq 0, \rho} \delta^\top \mathbf{H} \delta - \delta^\top \mathbf{f} + \frac{\mu}{2} \left\| \delta - \rho + \frac{1}{\mu} \boldsymbol{\eta} \right\|_2^2, \quad (27)$$

where the optimal solutions δ and ρ can be optimized alternately. The third term of the objective (27) is a penalty term which ensures $\delta = \rho$. The penalty factor $\mu > 0$ is gradually increased in each iteration. Meanwhile, $\boldsymbol{\eta} \in \mathbb{R}^V$ can be updated by $\boldsymbol{\eta} \leftarrow \boldsymbol{\eta} + \mu(\delta - \rho)$.

First, to update ρ with δ fixed, the Lagrange function w.r.t. ρ can be written as

$$\mathcal{L}(\rho) = \delta^{*\top} \mathbf{H} \rho + \frac{\mu}{2} \left\| \delta^* - \rho + \frac{1}{\mu} \boldsymbol{\eta} \right\|_2^2, \quad (28)$$

where δ is fixed with δ^* . By setting the derivative of $\mathcal{L}(\rho)$ w.r.t. ρ to zero, we can obtain the optimal solution as

$$\rho^* = \delta^* + \frac{1}{\mu} (\boldsymbol{\eta} - \mathbf{H}^\top \delta^*). \quad (29)$$

Second, to update δ with fixed ρ^* , the objective (27) can be transformed into solving the following problem

$$\min_{\delta^\top \mathbf{1}=1, \delta \geq 0} \left\| \delta - \rho^* + \frac{1}{\mu} (\boldsymbol{\eta} + \mathbf{H} \rho^* - \mathbf{f}) \right\|_2^2. \quad (30)$$

Thus, the problem (30) can be solved with a closed form solution according to [32].

For clarity, the overall algorithm of UDBGGL is described in Algorithm 1.

Algorithm 1 Multi-view clustering via unified and discrete bipartite graph learning (UDBGGL)

Input: Multi-view dataset $\{\mathbf{X}^{(v)}\}_{v=1}^V$, the number of clusters c , the number of anchors $m \geq c$, the parameters $\alpha > 0$ and $\beta > 0$.

Preparation: Normalize $\{\mathbf{X}^{(v)}\}_{v=1}^V$. Conduct k -means on the concatenated features $[\mathbf{X}^{(1)}; \mathbf{X}^{(2)}; \dots; \mathbf{X}^{(V)}]$ to obtain the anchors $[\mathbf{A}^{(1)}; \mathbf{A}^{(2)}; \dots; \mathbf{A}^{(V)}]$.

Initialization: $\delta = \mathbf{1}/V$. Initialize $\mathbf{Z}^{(v)}$ by K -nearest-neighbor (K -NN) bipartite graph.

```

1: repeat
2:   Initialize  $\gamma = 0.1$ ,  $\mathbf{D}_{(n)} = \text{diag}(\mathbf{B}\mathbf{1})$ , and  $\mathbf{D}_{(m)} = \text{diag}(\mathbf{B}^\top \mathbf{1})$ .
3:   Initialize  $\mathbf{F}$  by solving problem (13) (via replacing  $\mathbf{P}$  with  $\mathbf{B}$ ).
4:   repeat
5:     Update  $q_{ij} = \left\| \frac{\mathbf{F}_{(n)}(i,:)}{\sqrt{\mathbf{D}_{(n)}(i,i)}} - \frac{\mathbf{F}_{(m)}(j,:)}{\sqrt{\mathbf{D}_{(m)}(j,j)}} \right\|_2^2$ .
6:     Update  $\mathbf{P}$  by solving problem (18) and then update  $\mathbf{D}_s$ .
7:     Update  $\mathbf{F}$  by solving problem (13).
8:      $\text{temp} =$  the multiplicity of the eigenvalue 0 of  $\tilde{\mathbf{L}}_s$ .
9:     if  $\text{temp} < c$  then
10:        $\gamma \leftarrow 2\gamma$ .
11:     else if  $\text{temp} > c$  then
12:        $\gamma \leftarrow \gamma/2$ .
13:     end if
14:   until Obtaining the  $c$ -connected bipartite graph  $\mathbf{P}$ 
15:    $\forall v$ , update  $\mathbf{Z}^{(v)}$  by solving problem (19).
16:   Calculate  $\mathbf{H} = \hat{\mathbf{Z}}^\top \hat{\mathbf{Z}}$ , and  $\mathbf{f} = 2\hat{\mathbf{Z}}^\top \hat{\mathbf{p}}$ .
17:   Initialize  $\delta = \mathbf{1}/V$ ,  $\mu = 2$ , and  $\boldsymbol{\eta}$ .
18:   repeat
19:     Update  $\rho$  by Eq. (29).
20:     Update  $\delta$  by solving problem (30).
21:      $\boldsymbol{\eta} \leftarrow \boldsymbol{\eta} + \mu(\delta - \rho)$ ,  $\mu \leftarrow 2\mu$ .
22:   until  $\delta$  converges
23: until Convergence or maximum iteration reached

```

Output: The final clustering can be directly obtained from \mathbf{P} .

D. Computational Complexity Analysis

In this section, we analyze the computational complexity of the proposed algorithm. The computational cost of UDBGGL

TABLE II
DETAILS OF THE MULTI-VIEW DATASETS IN OUR EXPERIMENTS

Dataset	#Sample	#View	#Class	Dimension
WebKB-Texas	187	2	5	Citation(187), Content(1,703)
MSRCv1	210	4	7	CM(24), GIST(512), LBP(256), GENT(254)
Out-Scene	2,688	4	8	GIST(512), HOG(432), LBP(256), Gabor(48)
Cora	2,708	4	7	View1(2,708), View2(1,433), View3(2,708), View4(2,708)
Citeseer	3,312	2	6	Content(3,703), Citation(3,312)
VGGFace2	34,027	4	50	LBP(944), HOG(576), GIST(512), Gabor(640)
CIFAR-10	60,000	4	10	LBP(944), HOG(576), GIST(512), Gabor(640)
CIFAR-100	60,000	4	100	LBP(944), HOG(576), GIST(512), Gabor(640)

involves the computation of the preparation, the initialization, and the optimization of three variables. First, the normalization and the k -means take $\mathcal{O}(nd)$ and $\mathcal{O}(ndmt_1)$ time, respectively, where $d = \sum_v d^{(v)}$ and t_1 is the number of k -means iterations. Second, the cost of updating \mathbf{P} is $\mathcal{O}(nmct_2 + nm^2t_2 + m^3t_2)$, where t_2 is the iteration number of updating \mathbf{P} . Third, the cost of updating $\mathbf{Z}^{(v)}$ (for all v) is $\mathcal{O}(nm^2d)$. Finally, the cost of updating δ is $\mathcal{O}(V^2nm)$. Since $n \gg m$, and c, V, t_2 are small constants, the time complexity of UDBGL is linear in n .

V. EXPERIMENTS

In this section, we evaluate the proposed UDBGL method against the state-of-the-art MVC methods on eight multi-view datasets. All the experiments are conducted on a PC with 16GB RAM and an Intel i5-6600 CPU.

A. Datasets and Evaluation Metrics

In the experimental evaluation, eight real-world multi-view datasets are used, namely, WebKB-Texas [34], MSRCv1 [17], Out-Scene [35], Cora [36], Citeseer [36], VGGFace2¹, CIFAR-10, and CIFAR-100. Note that CIFAR-10 and CIFAR-100 are two versions of the CIFAR² dataset. The details of these benchmark datasets are given in Table II.

The clustering results are evaluated by three widely-used metrics, i.e., the normalized mutual information (NMI) [37], the accuracy (ACC) [38], and the purity (PUR) [27]. For all the three evaluation metrics, larger values indicate better clustering performance.

B. Baseline Methods and Experimental Settings

We experimentally compare the proposed UDBGL method against the eight baseline MVC methods, which are listed below.

- **MVSC** [18]: Large-scale multi-view spectral clustering via bipartite graph.
- **AMGL** [7]: Parameter-free auto-weighted multiple graph learning: a framework for multiview clustering and semi-supervised classification.
- **MLAN** [39]: Multi-view clustering and semi-supervised classification with adaptive neighbors.
- **SwMC** [2]: Self-weighted multiview clustering with multiple graphs.

- **SFMC** [22]: Multiview Clustering: A Scalable and Parameter-Free Bipartite Graph Fusion Method.
- **LMVSC** [27]: Large-scale multi-view subspace clustering in linear time.
- **SMVSC** [25]: Scalable multi-view subspace clustering with unified anchors.
- **FPMVS-CAG** [26]: Fast Parameter-Free Multi-View Subspace Clustering With Consensus Anchor Guidance.

Among these baseline MVC methods, AMGL, MLAN, and SwMC are three (conventional) graph learning based methods, while MVSC, SFMC, LMVSC, SMVSC, and FPMVS-CAG are five bipartite graph based methods which have better scalability for very large datasets.

For all test methods, the experiments are conducted 20 times, and the average scores and the standard deviations will be reported. The hyper-parameters in the proposed method and the baseline methods are tuned in the range of $\{10^{-5}, 10^{-4}, \dots, 10^5\}$, unless the value (or range) of the hyper-parameter is specified by the corresponding paper. The number of anchors is tuned in the range of $\{c, 50, 100, 200\}$. To avoid the expensive computational costs of parameter-tuning on the whole large-scale datasets, for all the test methods, if $n > 10,000$, then we will tune the hyper-parameters using a random subset of 10,000 samples.

C. Comparison with Other MVC Methods

In this section, we compare the proposed UDBGL method against the eight baseline MVC methods on the benchmark datasets. Specifically, the clustering scores w.r.t. NMI, ACC, and PUR by different methods are reported in Tables III, IV, and V, respectively. The best score on each dataset is highlighted in bold, and “N/A” indicates that this method is not computationally feasible on this dataset due to the out-of-memory error. As shown in Table III, in terms of NMI, our UDBGL method outperforms all baseline methods on seven out of the eight datasets. Though the FPMVS-CAG method yields a higher NMI score than UDBGL on the Out-Scene dataset, our UDBGL method outperforms FPMVS-CAG on all the other datasets. Similar advantages of UDBGL w.r.t. ACC and PUR can also be observed in Tables IV and V.

Further, we report the average scores and the average ranks (across all benchmark datasets) by different MVC methods in Tables III, IV, and V. Note that, among the nine MVC methods, if only five MVC methods are computational feasible and the other four methods are infeasible due to the out-of-memory error on a dataset, then the four infeasible methods will be equally ranked in the sixth position on this dataset.

¹https://www.robots.ox.ac.uk/~vgg/data/vgg_face2/

²<https://www.cs.toronto.edu/~kriz/cifar.html>

TABLE III
AVERAGE NMI(%) OVER 20 RUNS BY DIFFERENT MULTI-VIEW CLUSTERING METHODS. THE BEST RESULT IS HIGHLIGHTED IN **BOLD**.

Datasets	MVSC	AMGL	MLAN	SwMC	SFMC	LMVSC	SMVSC	FPMVS-CAG	UDBG
WebKB-Texas	1.98 \pm 0.25	9.89 \pm 2.61	7.11 \pm 1.72	9.37 \pm 0.00	6.25 \pm 0.00	20.20 \pm 0.00	21.42 \pm 0.00	22.76 \pm 0.00	37.14 \pm 0.00
MSRCv1	49.34 \pm 3.78	58.84 \pm 6.33	73.46 \pm 0.37	62.69 \pm 0.00	52.35 \pm 0.00	27.94 \pm 0.00	61.09 \pm 0.00	56.62 \pm 0.00	77.07 \pm 0.00
Out-Scene	23.39 \pm 14.73	44.19 \pm 3.96	37.38 \pm 0.00	43.69 \pm 0.00	39.72 \pm 0.00	45.97 \pm 0.00	51.67 \pm 0.00	53.04 \pm 0.00	52.92 \pm 0.00
Cora	0.25 \pm 0.09	9.00 \pm 4.79	2.55 \pm 0.00	8.69 \pm 0.01	4.79 \pm 0.00	21.45 \pm 0.00	28.73 \pm 0.00	18.19 \pm 0.00	36.97 \pm 0.00
Citeseer	0.40 \pm 0.11	0.53 \pm 0.06	1.85 \pm 4.51	1.22 \pm 0.00	2.43 \pm 0.00	8.75 \pm 0.00	17.86 \pm 0.00	14.73 \pm 0.00	26.06 \pm 0.00
VGGFace2	N/A	N/A	N/A	N/A	7.79 \pm 0.00	13.62 \pm 0.00	11.16 \pm 0.00	12.33 \pm 0.00	14.27 \pm 0.00
CIFAR-10	N/A	N/A	N/A	N/A	1.76 \pm 0.00	13.54 \pm 0.00	18.37 \pm 0.00	18.41 \pm 0.00	19.60 \pm 0.00
CIFAR-100	N/A	N/A	N/A	N/A	12.25 \pm 0.00	14.50 \pm 0.00	13.93 \pm 0.00	13.75 \pm 0.00	14.89 \pm 0.00
Avg.score	-	-	-	-	15.92	20.75	28.03	26.23	34.87
Avg.rank	7.75	5.75	6.13	5.75	6.13	4.00	3.00	3.13	1.13

* Note that N/A indicates the out-of-memory error, and the symbol “-” indicates that the average score cannot be calculated.

TABLE IV
AVERAGE ACC(%) OVER 20 RUNS BY DIFFERENT MULTI-VIEW CLUSTERING METHODS. THE BEST RESULT IS HIGHLIGHTED IN **BOLD**.

Datasets	MVSC	AMGL	MLAN	SwMC	SFMC	LMVSC	SMVSC	FPMVS-CAG	UDBG
WebKB-Texas	55.13 \pm 0.30	51.79 \pm 5.36	49.63 \pm 0.59	54.55 \pm 0.00	40.11 \pm 0.00	60.43 \pm 0.00	56.68 \pm 0.00	57.75 \pm 0.00	69.52 \pm 0.00
MSRCv1	56.98 \pm 5.33	64.90 \pm 8.10	73.81 \pm 0.00	70.48 \pm 0.00	56.67 \pm 0.00	36.67 \pm 0.00	67.14 \pm 0.00	60.00 \pm 0.00	74.76 \pm 0.00
Out-Scene	31.82 \pm 10.36	49.91 \pm 5.12	40.55 \pm 0.00	45.46 \pm 0.00	47.84 \pm 0.00	59.86 \pm 0.00	63.32 \pm 0.00	63.58 \pm 0.00	68.01 \pm 0.00
Cora	30.19 \pm 0.11	33.58 \pm 3.00	31.39 \pm 0.00	34.46 \pm 0.13	28.32 \pm 0.00	40.84 \pm 0.00	53.29 \pm 0.00	44.53 \pm 0.00	52.66 \pm 0.00
Citeseer	21.24 \pm 0.17	21.48 \pm 0.06	22.64 \pm 4.29	21.62 \pm 0.00	24.67 \pm 0.00	29.35 \pm 0.00	41.94 \pm 0.00	37.53 \pm 0.00	50.39 \pm 0.00
VGGFace2	N/A	N/A	N/A	N/A	8.11 \pm 0.00	11.55 \pm 0.00	9.83 \pm 0.00	10.74 \pm 0.00	12.31 \pm 0.00
CIFAR-10	N/A	N/A	N/A	N/A	11.52 \pm 0.00	25.81 \pm 0.00	29.20 \pm 0.00	29.55 \pm 0.00	29.84 \pm 0.00
CIFAR-100	N/A	N/A	N/A	N/A	6.87 \pm 0.00	7.96 \pm 0.00	8.14 \pm 0.00	9.06 \pm 0.00	9.05 \pm 0.00
Avg.score	-	-	-	-	28.01	34.06	41.19	39.09	45.82
Avg.rank	7.00	6.13	6.13	5.75	6.50	4.13	3.00	2.88	1.25

* Note that N/A indicates the out-of-memory error, and the symbol “-” indicates that the average score cannot be calculated.

TABLE V
AVERAGE PUR(%) OVER 20 RUNS BY DIFFERENT MULTI-VIEW CLUSTERING METHODS. THE BEST RESULT IS HIGHLIGHTED IN **BOLD**.

Datasets	MVSC	AMGL	MLAN	SwMC	SFMC	LMVSC	SMVSC	FPMVS-CAG	UDBG
WebKB-Texas	56.10 \pm 0.16	60.00 \pm 1.98	56.58 \pm 0.88	59.89 \pm 0.00	55.61 \pm 0.00	62.57 \pm 0.00	67.91 \pm 0.00	65.78 \pm 0.00	72.73 \pm 0.00
MSRCv1	59.31 \pm 5.06	68.10 \pm 7.17	80.48 \pm 0.00	73.33 \pm 0.00	59.52 \pm 0.00	40.95 \pm 0.00	69.05 \pm 0.00	62.86 \pm 0.00	80.48 \pm 0.00
Out-Scene	32.03 \pm 10.40	50.47 \pm 5.32	40.85 \pm 0.00	45.57 \pm 0.00	48.21 \pm 0.00	59.86 \pm 0.00	66.00 \pm 0.00	67.08 \pm 0.00	68.01 \pm 0.00
Cora	30.34 \pm 0.08	35.54 \pm 3.03	31.79 \pm 0.00	36.70 \pm 0.09	32.90 \pm 0.00	45.86 \pm 0.00	53.66 \pm 0.00	45.49 \pm 0.00	59.19 \pm 0.00
Citeseer	21.39 \pm 0.11	21.57 \pm 0.05	22.80 \pm 4.39	22.04 \pm 0.00	25.30 \pm 0.00	31.76 \pm 0.00	47.01 \pm 0.00	42.81 \pm 0.00	52.57 \pm 0.00
VGGFace2	N/A	N/A	N/A	N/A	8.52 \pm 0.00	12.29 \pm 0.00	10.28 \pm 0.00	11.15 \pm 0.00	13.29 \pm 0.00
CIFAR-10	N/A	N/A	N/A	N/A	11.92 \pm 0.00	27.48 \pm 0.00	32.40 \pm 0.00	32.85 \pm 0.00	31.61 \pm 0.00
CIFAR-100	N/A	N/A	N/A	N/A	7.57 \pm 0.00	9.37 \pm 0.00	8.64 \pm 0.00	9.45 \pm 0.00	9.83 \pm 0.00
Avg.score	-	-	-	-	31.19	36.27	44.37	42.18	48.46
Avg.rank	7.63	5.88	6.00	5.75	6.13	4.13	2.88	3.00	1.25

* Note that N/A indicates the out-of-memory error, and the symbol “-” indicates that the average score cannot be calculated.

In terms of the average score, UDBG achieves the average NMI(%), ACC(%), and PUR(%) scores of 34.87, 45.82, 48.46, respectively, which substantially outperforms the second best average NMI(%), ACC(%), and PUR(%) scores of 28.03, 41.19, and 44.37, respectively. In terms of the average rank, UDBG obtains the average ranks (w.r.t. NMI, ACC, and PUR) of 1.13, 1.25, and 1.25, respectively, while the second best method only obtains the average ranks of 3.00, 2.88, and 2.88, respectively, which show the robustness of the proposed UDBG method over the other MVC methods.

D. Parameter Analysis

In this section, we test the influence of the parameters α and β in our UDBG method. In UDBG, the two balance

parameters, i.e., α and β , are utilized to negotiate the importance of the regularization term (of $\mathbf{Z}^{(v)}$) and the graph fusion term. The performance of UDBG with varying hyperparameters α and β is illustrated in Fig. 2, which suggests that moderate parameter values are generally beneficial to the clustering performance on different datasets.

E. Convergence Analysis

In this section, we test the convergence of UDBG on the benchmark datasets. Fig. 3 shows the convergence curves of the objective function values of UDBG after different iterations. As can be seen in Fig. 3, the objective function value decreases very fast and generally converges within

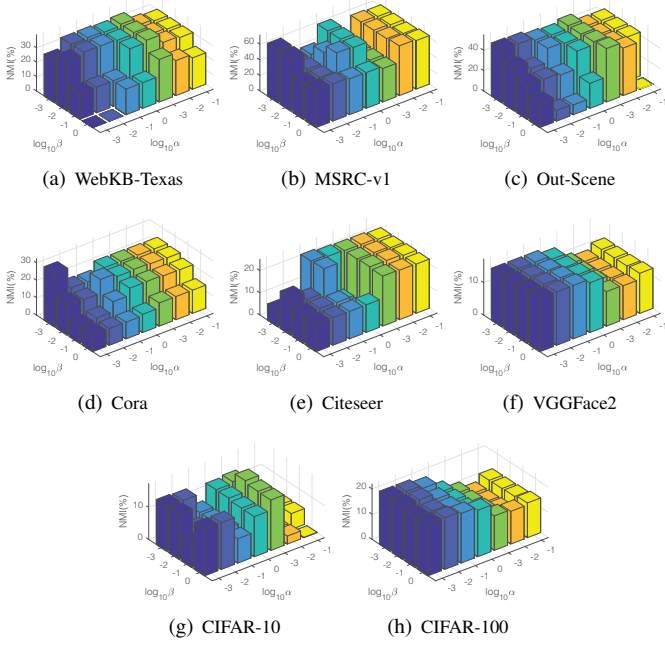


Fig. 2. The clustering performance (w.r.t. NMI) by UDBGL with varying values of parameters α and β .

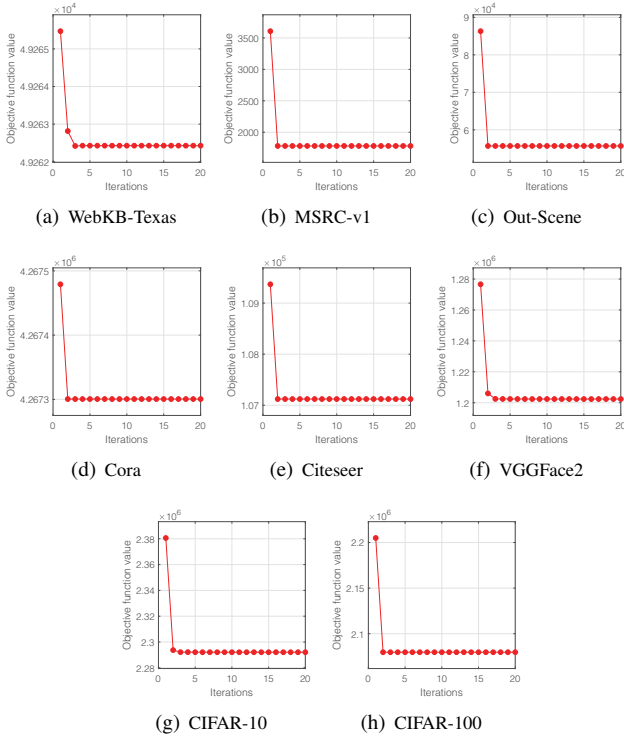


Fig. 3. Convergence of the objective value of UDBGL with increasing iterations.

twenty iterations on various datasets, which shows the good convergence property of the proposed UDBGL method.

F. Ablation Study

To verify the contributions of the regularization term of $\mathbf{Z}^{(v)}$ and the bipartite graph fusion term, we report and analyze the ablation results in this section.

TABLE VI
ABLATION ANALYSIS ON THE BENCHMARK DATASETS. THE BEST SCORE IN EACH ROW IS HIGHLIGHTED IN BOLD.

Method		Ablation			UDBGL
Regularization of $\mathbf{Z}^{(v)}$		✗	✓	✗	✓
Bipartite Graph Fusion		✗	✗	✓	✓
WebKB-Texas	NMI	14.94	15.19	15.73	37.14
	ACC	26.20	25.94	30.48	69.52
	PUR	36.36	34.49	35.83	72.73
MSRCv1	NMI	33.97	34.24	33.87	77.07
	ACC	37.14	37.38	37.86	74.76
	PUR	39.52	39.76	39.76	80.48
Out-Scene	NMI	25.81	27.62	26.41	52.92
	ACC	33.89	34.47	33.95	68.01
	PUR	33.89	34.47	33.95	68.01
Cora	NMI	9.26	12.54	16.31	36.97
	ACC	19.87	19.66	24.50	52.66
	PUR	22.36	24.52	28.23	59.19
Citeseer	NMI	12.72	14.59	13.04	26.06
	ACC	25.08	27.70	25.20	50.39
	PUR	26.10	29.27	26.28	52.57
VGGFace2	NMI	6.75	7.31	7.11	14.27
	ACC	5.97	6.50	6.13	12.31
	PUR	6.38	6.82	6.63	13.29
CIFAR-10	NMI	8.83	9.55	9.39	19.60
	ACC	14.64	15.26	14.61	29.84
	PUR	16.20	17.21	15.97	31.61
CIFAR-100	NMI	8.33	9.35	7.45	14.89
	ACC	4.70	5.43	4.52	9.05
	PUR	5.49	6.43	4.91	9.83

Note that our UDBGL method directly obtains a unified bipartite graph with c clusters through the bipartite graph fusion term. If this fusion term is removed, then we need extra post-processing to gain the clustering result. Specifically, in the case of removing the fusion term, we compute the c left singular vectors (corresponding to the largest c eigenvalues) of the concatenated bipartite graph $\bar{\mathbf{Z}} = (1/\sqrt{V})[\mathbf{Z}^{(1)}, \mathbf{Z}^{(2)}, \dots, \mathbf{Z}^{(V)}]$ to obtain the spectral embedding $\bar{\mathbf{U}}$, and perform the k -means on $\bar{\mathbf{U}}$ to achieve the final clustering like LMVSC [27]. The comparison results in Table VI have shown the substantial contributions of the regularization term of $\mathbf{Z}^{(v)}$ and the bipartite graph fusion term, while removing each of them may lead to performance degradation.

G. Execution Time

In this section, we report the execution times of the proposed method and the baseline methods on the six larger datasets (with $n > 2,000$). As shown in Fig. 4, the MVSC, AMGL, MLAN, and SwMC methods are not computationally feasible on the three large-scale datasets (with over 30,000 samples), while the other five bipartite graph based methods are computationally feasible on all the datasets. Typically, the proposed UDBGL method has shown comparable time cost to the SMVSC and FPMVS-CAG methods on most of the benchmark datasets.

From the performance results in Tables III, IV, and V and the execution times in Fig. 4, we can observe that our UDBGL method is able to achieve advantageous clustering performance on various datasets while maintaining competitive efficiency.

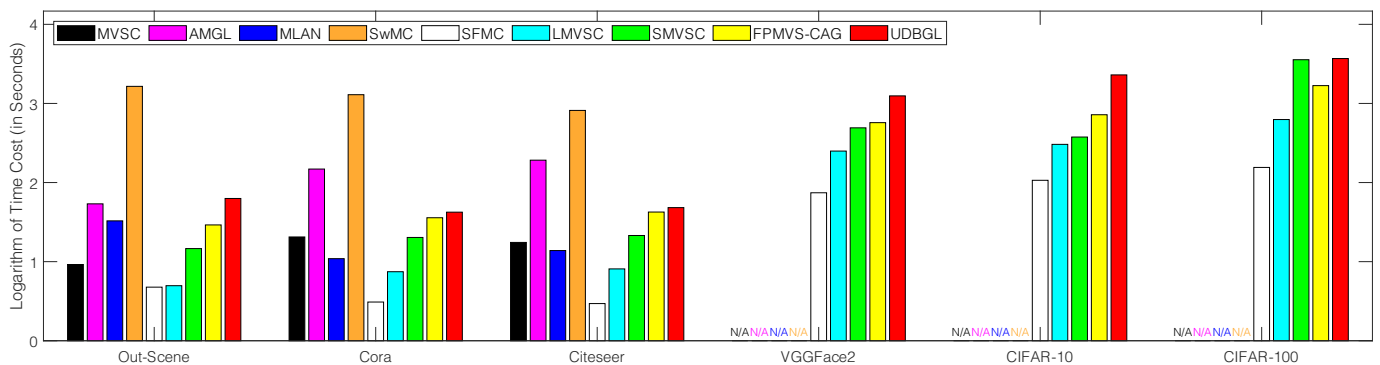


Fig. 4. Execution times of different MVC methods on the six larger datasets (with $n > 2,000$). Note that N/A indicates the out-of-memory error.

VI. CONCLUSION

In this paper, we propose an efficient MVC approach termed UDBGL. In particular, the anchor-based subspace learning is enforced to learn the view-specific bipartite graphs from multiple views, which are fused into a view-consensus bipartite graph with adaptive view weights. Remarkably, the view-specific bipartite graph learning and the view-consensus bipartite graph learning can promote each other mutually and adaptively, which are further coupled with the Laplacian low rank constraint to directly obtain the discrete cluster structure from the fused graph. An alternating minimization algorithm is designed to optimize the proposed model, whose computational complexity is linear to the data size. Extensive experiments on eight multi-view datasets, whose data sizes range from 187 to 60,000, have demonstrated the clustering robustness and efficiency of our UDBGL approach over the state-of-the-art MVC approaches.

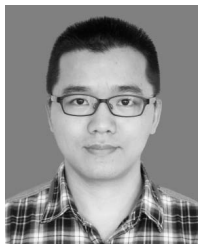
REFERENCES

- [1] G. Chao, S. Sun, and J. Bi, "A survey on multiview clustering," *IEEE Transactions on Artificial Intelligence*, vol. 2, no. 2, pp. 146–168, 2021.
- [2] F. Nie, J. Li, X. Li *et al.*, "Self-weighted multiview clustering with multiple graphs," in *Proc. of International Joint Conference on Artificial Intelligence (IJCAI)*, 2017, pp. 2564–2570.
- [3] K. Zhan, F. Nie, J. Wang, and Y. Yang, "Multiview consensus graph clustering," *IEEE Transactions on Image Processing*, vol. 28, no. 3, pp. 1261–1270, 2018.
- [4] H. Wang, Y. Yang, and B. Liu, "Gmc: Graph-based multi-view clustering," *IEEE Transactions on Knowledge and Data Engineering*, vol. 32, no. 6, pp. 1116–1129, 2019.
- [5] Y. Liang, D. Huang, C.-D. Wang, and P. S. Yu, "Multi-view graph learning by joint modeling of consistency and inconsistency," *IEEE Transactions on Neural Networks and Learning Systems*, 2022.
- [6] W. Liang, X. Liu, S. Zhou, J. Liu, S. Wang, and E. Zhu, "Robust graph-based multi-view clustering," in *Proc. of AAAI Conference on Artificial Intelligence*, 2022, pp. 7462–7469.
- [7] F. Nie, J. Li, X. Li *et al.*, "Parameter-free auto-weighted multiple graph learning: a framework for multiview clustering and semi-supervised classification," in *Proc. of International Joint Conference on Artificial Intelligence (IJCAI)*, 2016, pp. 1881–1887.
- [8] X.-L. Li, M.-S. Chen, C.-D. Wang, and J.-H. Lai, "Refining graph structure for incomplete multi-view clustering," *IEEE Transactions on Neural Networks and Learning Systems*, 2022.
- [9] Y. Liang, D. Huang, and C.-D. Wang, "Consistency meets inconsistency: A unified graph learning framework for multi-view clustering," in *Proc. of IEEE International Conference on Data Mining (ICDM)*, 2019, pp. 1204–1209.
- [10] H. Gao, F. Nie, X. Li, and H. Huang, "Multi-view subspace clustering," in *Proc. of IEEE International Conference on Computer Vision (ICC)*, 2015, pp. 4238–4246.
- [11] C. Zhang, Q. Hu, H. Fu, P. Zhu, and X. Cao, "Latent multi-view subspace clustering," in *Proc. of IEEE Conference on Computer Vision and Pattern Recognition (CVPR)*, 2017, pp. 4279–4287.
- [12] R. Vidal, "Subspace clustering," *IEEE Signal Processing Magazine*, vol. 28, no. 2, pp. 52–68, 2011.
- [13] G.-Y. Zhang, Y.-R. Zhou, X.-Y. He, C.-D. Wang, and D. Huang, "One-step kernel multi-view subspace clustering," *Knowledge-Based Systems*, vol. 189, p. 105126, 2020.
- [14] C. Tang, X. Zhu, X. Liu, M. Li, P. Wang, C. Zhang, and L. Wang, "Learning a joint affinity graph for multiview subspace clustering," *IEEE Transactions on Multimedia*, vol. 21, no. 7, pp. 1724–1736, 2019.
- [15] Z. Kang, X. Zhao, C. Peng, H. Zhu, J. T. Zhou, X. Peng, W. Chen, and Z. Xu, "Partition level multiview subspace clustering," *Neural Networks*, vol. 122, pp. 279–288, 2020.
- [16] X. Cao, C. Zhang, H. Fu, S. Liu, and H. Zhang, "Diversity-induced multi-view subspace clustering," in *Proc. of IEEE Conference on Computer Vision and Pattern Recognition (CVPR)*, 2015, pp. 586–594.
- [17] M.-S. Chen, L. Huang, C.-D. Wang, and D. Huang, "Multi-view clustering in latent embedding space," in *Proc. of AAAI conference on artificial intelligence*, vol. 34, no. 04, 2020, pp. 3513–3520.
- [18] Y. Li, F. Nie, H. Huang, and J. Huang, "Large-scale multi-view spectral clustering via bipartite graph," in *Proc. of AAAI Conference on Artificial Intelligence*, 2015.
- [19] F. Nie, X. Wang, C. Deng, and H. Huang, "Learning a structured optimal bipartite graph for co-clustering," *Advances in Neural Information Processing Systems (NeurIPS)*, vol. 30, 2017.
- [20] J. Guo and J. Ye, "Anchors bring ease: An embarrassingly simple approach to partial multi-view clustering," in *Proc. of AAAI Conference on Artificial Intelligence*, vol. 33, no. 01, 2019, pp. 118–125.
- [21] L. Li and H. He, "Bipartite graph based multi-view clustering," *IEEE Transactions on Knowledge and Data Engineering*, 2020.
- [22] X. Li, H. Zhang, R. Wang, and F. Nie, "Multiview clustering: A scalable and parameter-free bipartite graph fusion method," *IEEE Transactions on Pattern Analysis and Machine Intelligence*, vol. 44, no. 1, pp. 330–344, 2020.
- [23] Z. Kang, Z. Lin, X. Zhu, and W. Xu, "Structured graph learning for scalable subspace clustering: From single view to multiview," *IEEE Transactions on Cybernetics*, vol. 52, no. 9, pp. 8976–8986, 2022.
- [24] F. Nie, W. Chang, R. Wang, and X. Li, "Learning an optimal bipartite graph for subspace clustering via constrained laplacian rank," *IEEE Transactions on Cybernetics*, 2021.
- [25] M. Sun, P. Zhang, S. Wang, S. Zhou, W. Tu, X. Liu, E. Zhu, and C. Wang, "Scalable multi-view subspace clustering with unified anchors," in *Proc. of ACM International Conference on Multimedia (ACM MM)*, 2021, pp. 3528–3536.
- [26] S. Wang, X. Liu, X. Zhu, P. Zhang, Y. Zhang, F. Gao, and E. Zhu, "Fast parameter-free multi-view subspace clustering with consensus anchor guidance," *IEEE Transactions on Image Processing*, vol. 31, pp. 556–568, 2021.
- [27] Z. Kang, W. Zhou, Z. Zhao, J. Shao, M. Han, and Z. Xu, "Large-scale multi-view subspace clustering in linear time," in *Proc. of AAAI conference on Artificial Intelligence*, vol. 34, no. 04, 2020, pp. 4412–4419.

- [28] X. Lu and S. Feng, "Structure diversity-induced anchor graph fusion for multi-view clustering," *ACM Transactions on Knowledge Discovery from Data*, 2022.
- [29] W. Liu, J. He, and S.-F. Chang, "Large graph construction for scalable semi-supervised learning," in *Proc. of International Conference on Machine Learning (ICML)*, 2010.
- [30] U. Von Luxburg, "A tutorial on spectral clustering," *Statistics and Computing*, vol. 17, no. 4, pp. 395–416, 2007.
- [31] K. Fan, "On a theorem of weyl concerning eigenvalues of linear transformations i," *Proceedings of the National Academy of Sciences of the United States of America*, vol. 35, no. 11, p. 652, 1949.
- [32] J. Huang, F. Nie, and H. Huang, "A new simplex sparse learning model to measure data similarity for clustering," in *Proc. of International Joint Conference on Artificial Intelligence (IJCAI)*, 2015.
- [33] D. P. Bertsekas, "Constrained optimization and lagrange multiplier methods," *Computer Science and Applied Mathematics*, 1982.
- [34] M. Craven, A. McCallum, D. PiPasquo, T. Mitchell, and D. Freitag, "Learning to extract symbolic knowledge from the world wide web," Carnegie-mellon univ pittsburgh pa school of computer Science, Tech. Rep., 1998.
- [35] Z. Hu, F. Nie, R. Wang, and X. Li, "Multi-view spectral clustering via integrating nonnegative embedding and spectral embedding," *Information Fusion*, vol. 55, pp. 251–259, 2020.
- [36] X. Liu, L. Liu, Q. Liao, S. Wang, Y. Zhang, W. Tu, C. Tang, J. Liu, and E. Zhu, "One pass late fusion multi-view clustering," in *Proc. of International Conference on Machine Learning (ICML)*, 2021, pp. 6850–6859.
- [37] D. Huang, C.-D. Wang, J.-H. Lai, and C.-K. Kwok, "Toward multidiversified ensemble clustering of high-dimensional data: From subspaces to metrics and beyond," *IEEE Transactions on Cybernetics*, 2021.
- [38] D. Huang, C.-D. Wang, J.-S. Wu, J.-H. Lai, and C.-K. Kwok, "Ultra-scalable spectral clustering and ensemble clustering," *IEEE Transactions on Knowledge and Data Engineering*, vol. 32, no. 6, pp. 1212–1226, 2019.
- [39] F. Nie, G. Cai, and X. Li, "Multi-view clustering and semi-supervised classification with adaptive neighbours," in *Proc. of AAAI Conference on Artificial Intelligence*, 2017.



Siguo Fang received the B.S. degree in information and computing sciences from the China Jiliang University, Hangzhou, China, in 2021. He is currently pursuing the master degree in computer science with the College of Mathematics and Informatics, South China Agricultural University, Guangzhou, China. His research interests include multi-view clustering and large-scale clustering.



Dong Huang received the B.S. degree in computer science in 2009 from South China University of Technology, Guangzhou, China. He received the M.Sc. degree in computer science in 2011 and the Ph.D. degree in computer science in 2015, both from Sun Yat-sen University, Guangzhou, China. He joined South China Agricultural University in 2015, where he is currently an Associate Professor with the College of Mathematics and Informatics. From July 2017 to July 2018, he was a visiting fellow with the School of Computer Science and Engineering, Nanyang Technological University, Singapore. His research interests include data mining and machine learning. He has published more than 60 papers in international journals and conferences, such as IEEE TKDE, IEEE TNNLS, IEEE TCYB, IEEE TSMC-S, ACM TKDD, SIGKDD, AAAI, and ICDM. He was the recipient of the 2020 ACM Guangzhou Rising Star Award.



Xiao-Sha Cai received her B.S. degree in software engineering in 2019 and her M.Sc. degree in computer science in 2022, both from South China Agricultural University, Guangzhou, China. She is currently pursuing her Ph.D degree at Sun Yat-sen University, Guangzhou, China. Her research interests include data clustering and information fusion.



Chang-Dong Wang received the B.S. degree in applied mathematics in 2008, the M.Sc. degree in computer science in 2010, and the Ph.D. degree in computer science in 2013, all from Sun Yat-sen University, Guangzhou, China. He was a visiting student at the University of Illinois at Chicago from January 2012 to November 2012. He is currently an Associate Professor with the School of Data and Computer Science, Sun Yat-sen University, Guangzhou, China. His current research interests include machine learning and data mining. He has published more than 100 scientific papers in international journals and conferences such as IEEE TPAMI, IEEE TKDE, IEEE TNNLS, IEEE TSMC-C, ACM TKDD, Pattern Recognition, SIGKDD, ICDM and SDM. His ICDM 2010 paper won the Honorable Mention for Best Research Paper Award. He was awarded 2015 Chinese Association for Artificial Intelligence (CAAI) Outstanding Dissertation.



Chaobo He received his Ph.D., M.S., and B.S. degrees from South China Normal University, Guangzhou, China, in 2014, 2007, and 2004, respectively. He is currently a Professor with the School of Computer Science, South China Normal University. His research interests are data mining and social computing. He has published over 30 papers in international journals and conferences.



Yong Tang is the founder of SCHOLAT, a kind of scholar social network. He is now a Professor and Dean of School of Computer Science at South China Normal University. He got his BS and MSc degrees from Wuhan University in 1985 and 1990 respectively, and PhD degree from University of Science and Technology of China in 2001, all in computer science. Before joining South China Normal University in 2009, he was vice Dean of School of Information of Science and Technology at Sun Yat-Sen University. He has published more than 200 papers and books. He has supervised more than 40 PhD students since 2003 and more than 100 Master students since 1996. His main research areas include data and knowledge engineering, social networking and collaborative computing. He currently serves as the director of technical committee on collaborative computing of China Computer Federation (CCF) and the executive vice president of Guangdong Computer Academy. For more information, please visit <https://scholat.com/ytang>.